# Global Water Resources Assessment and Future Projections

Katumi Musiake, Taikan Oki, Yasushi Agata and Shinjiro Kanae

## Abstract

Anticipated water scarcity in the first half of this century is one of the major causes for concern among international issues. However, even though the issue has an international impact and worldwide monitoring is critical, the number of global estimates at present and future projections are limited.

In this study, annual water availability was derived from annual runoff estimated by land surface models using Total Runoff Integrating Pathways (TRIP) with 0.5° by 0.5° longitude/latitude resolution globally. Global distribution of water withdrawal for each sector in the same horizontal spatial resolution was estimated based on country statistics of municipal water use, industrial water use, and agricultural intake, using global geographical information systems with global distribution of population and irrigated crop land area.

Although the total population under water stress estimated for 1995 corresponded very well to former estimates, the number highly depended on how to determine the ratio indicating how much water from outside of a region can be used for water resources within a region. This suggests the importance of regional studies for evaluating the possibility of water intake as well as the validity of the investment for water resources withdrawal facilities.

Based on the assessment of the current situation, projections for 2050 were derived considering the effects of climate change and population growth. The effect of climate change on water resources was derived from the changes in runoff in a global warming simulation conducted by the Center for Climate System Research, University of Tokyo. The population growth followed the scenario developed by the United Nations.

As a result, water resources and water stress in 2050 were estimated. The changes in the geographical distribution of water stress between 1995 and 2050 did not seem to be apparent at a glance. However, instead of obvious changes, the projection indicated that the regions affected by severe stress in 1995 will experience more severe stress and that these regions will spread to neighboring regions. It can be argued that water scarcity has already been emerging in certain regions in the world and such regions themselves might face a more serious situation in the future, and that population growth in the future will exert a major effect on water scarcity compared to climate change.

## 1 Introduction

It is anticipated that the world's water resources will be under more pressure in the first half of this century than at any time during the recorded history. The estimation of the current level of water stress is important for reliable projections of the severity of the water-crisis in the future. However, most of the previous global analyses on water scarcity have been carried out on a country basis or a river basin basis

---

Institute of Industrial Science, University of Tokyo, 4-6-1 Komaba, Meguro-ku, Tokyo 153-8505, Japan.

with the exceptions of Takahashi *et al.* (2000) and Vörösmarty *et al.* (2000), who analyzed water scarcity in 0.5° by 0.5° longitude and latitude grid boxes for the globe. Considering the importance of global water scarcity, future projections should be evaluated by multiple procedures/models/methods in various organizations, since the reliability of the estimates will be supported if similar results are obtained from different scientific approaches, information, and data processing.

For the global estimation of the water supply, observed runoff or simulated runoff is generally used. Shiklomanov (2000a; 2000b) estimated the water availability for 26 regions of the world based on observed river discharge at 2,500 stations. Takahashi *et al.* (2000) estimated the monthly water balance in 0.5° by 0.5° longitude/latitude grid boxes using a bucket model (Manabe, 1969) with potential evapotranspiration by the Penman method using current and future climate projections (temperature, wind speed, and precipitation) simulated by GCMs (General Circulation Models) of the Canadian Climate Centre, Max Planck Institute, and Center for Climate System Research (CCSR), University of Tokyo. Vörösmarty *et al.* (2000) adopted a similar approach, but their water supply estimates were linearly adjusted to observations where discharge information was available. In this study, the water balance estimated based on land surface models (LSMs) was used for the global estimates of water availability. Such models were originally developed to be included in numerical atmospheric models to compute the lower boundary condition of the atmospheric circulation. The bucket model (Manabe, 1969) is the first generation LSM and is relatively simple. However, current LSMs consider detailed energy and water balances at the land surface including hydrological, radiative, and even biogeochemical processes. All the GCMs that provide future climate projections use some kind of LSMs. Since current LSMs can simulate monthly scale river runoff considerably well, provided that the precipitation and other forcing input data for the LSMs are accurate enough (Oki *et al.*, 1999), it is highly possible that LSMs will be directly used for the water resources projections in the future when GCMs will simulate the hydrological cycles with enough accuracy. Therefore it is worthwhile to apply the current global water balances calculated based on LSMs for the current water resources assessments. The methodology and results are presented in Section 2.

For the demand side of water resources assessments, two kinds of distributed information can be used globally in 0.5° by 0.5° longitude/latitude grid boxes; namely population and irrigated land area. In this study, country-based statistics, such as municipal water supply and industrial water use are assumed to be proportional to the population distribution, and agricultural intake is assumed to be proportional to the irrigated land area. A Global Geographical Information System (G-GIS) was developed to convert country-based statistics into grid-based global distribution. Statistics were given for various "current" years, and all of the statistics were linearly adjusted to the year 1995. The target year was selected partly in order to compare the results with previous global estimates by UN *et al.* (1997), Vörösmarty *et al.* (2000), but mainly because the latest information globally available when the assessment started was mostly in 1995.

From these estimates of global annual water supply and demand, the global distribution of water stress was estimated for every 0.5° by 0.5° longitude/latitude grid boxes. The results were compared with previous estimates on country-, river basin-, and grid-basis in Section 4.


## 2 Water availability estimated by TRIP

Simulated runoff values from offline runs with 10 different LSMs were used for estimating water availability in this study. Under the Global Soil Wetness Project (GSWP; IGPO (1995)), the global water balance was estimated by 11 LSMs using forcing data, such as precipitation, downward short wave and long wave radiation, wind speed, temperature, humidity, and surface pressure, from ISLSCP (International Satellite Land Surface Climatology Project) (Meeson *et al.*, 1995). Surface runoff values estimated by CCSR (Center for

Climate System Research, Univ. of Tokyo)-Bucket (Numaguti *et al.*, 1997) and JMA (Japan Meteorological Agency)-SiB (Sato *et al.*, 1989) models were sent to the Data Center of the GSWP. Therefore the average values of these two estimates were used for the surface runoff. As for the total runoff, the average values of the estimates by all the 11 LSMs were utilized. The target period of the GSWP was from 1987 through 1988, and the surface and total runoff were produced approximately every 10 days in 1° by 1° grid boxes.

To estimate the river discharge, the gridded surface and total runoff data were divided into 0.5° longitude/latitude resolution and TRIP (Total Runoff Integrating Pathways) (Oki and Sud, 1998) corresponding to the horizontal resolution was used to determine the flow direction globally. Flow routing was improved from a simple linear scheme (Oki *et al.*, 1999) using a system similar to that of Arora *et al.* (1999). The governing equations were the continuity equation of water mass in the grid box and Manning's equation.

Firstly, the groundwater was represented by a simple linear reservoir.

$$\frac{dS_g}{dt} = D_{LSMg} - D_{OUTg} \tag{1}$$

where, $S_g$, $D_{LSMg}$, $D_{OUTg}$ are the groundwater storage, inflow from LSM substituted for the amount of surface runoff, and the outflow from the groundwater reservoir, respectively. The outflow was parameterized as:

$$D_{OUTg} = \frac{1}{\tau} S_g \tag{2}$$

where $\tau$ is the time constant. Globally $\tau = 30$ [days] was assumed in this study.

## TRIP Annual River Discharge
### [$10^6$ m³/year/0.5°grid]
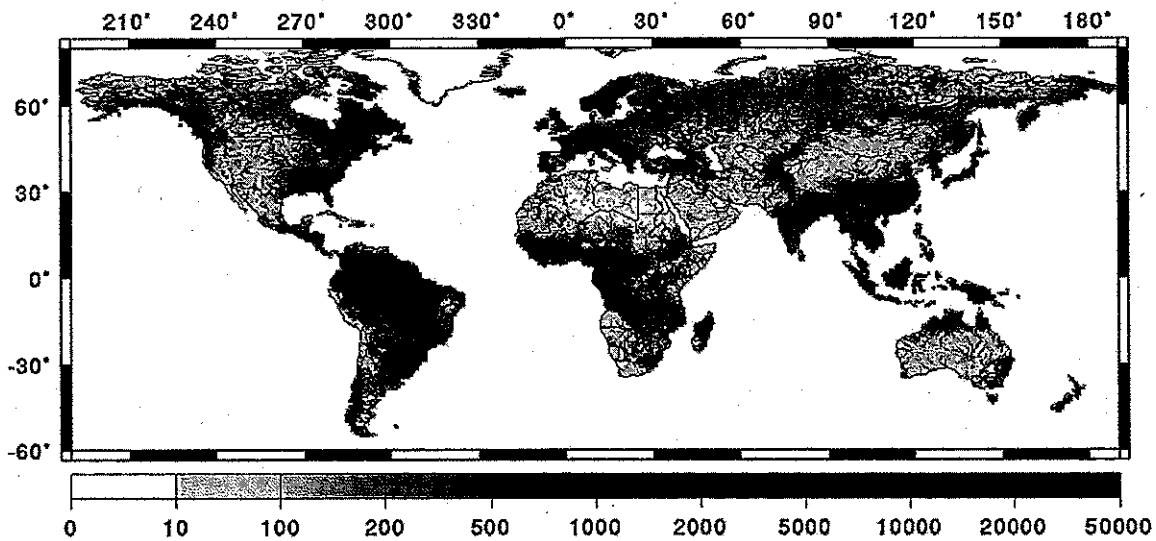#### (Average of 1987 and 1988)



**Fig. 1   Estimated annual total river discharge in each 0.5° x 0.5° lon./lat. grid box**

The continuity equation for water in the river channel was:

$$\frac{dS_{rc}}{dt} = D_{IN} + D_{OUTg} + D_{LSMs} - D_{OUT} \tag{3}$$

where $S_{rc}$, $D_{IN}$, $D_{LSMs}$, and $D_{OUT}$ are the water in the river channel, total inflow from surrounding grid boxes, surface runoff calculated based on LSMs, and outflow from the grid box, respectively. Assuming that the

width and depth of the river channel are $w$ and $h$, outflow is $D_{OUT} = hwv$ where $v$ is the flow velocity. For a large river channel, Manning's equation can be written as:

$$v = \frac{1}{n} h^{2/3} I^{1/2} \tag{4}$$

where $n$ is the Manning's coefficient and $I$ is the slope. In this study $n$ is assumed to be 0.045 globally, which is within the range of the values for meandering river channels.

Volume of water in the river channel was:

$$S_{rc} = w \times h \times l \times r_M \tag{5}$$

where $l$ is the straight length of the river channel within the grid box calculated geometrically and $r_M$ (=1.4 globally) is the meandering ratio (Oki and Sud, 1998) used to adjust the river length to a realistic value. To obtain $h$, information on $w$ should be given. Applying an empirical function to the relationship between the annual mean discharge $Q_M$ (m³ /s) and river width $w$ (m) (Leopold, 1996),

$$w = (100.9 \times Q_M)^{0.4856} \tag{6}$$

was empirically obtained. The tentative annual mean discharge $Q_M$ was calculated with effective velocity $v_e$ =0.5 [m/s] globally, and river width $w$ in each grid box was determined by equation (6) by setting the minimum $w$ value to be 10 [m]. From these calculations, the maximum river width was estimated at nearly 3 km. The slope $I$ was determined from a digital elevation model (DEM) by setting the minimum slope at $10^5$.

Figure 1 illustrates the annual total river discharge in each 0.5° by 0.5° longitude/latitude grid box. The average of estimates for 1987 and 1988 is presented and considered as the available water resources for 1995 in the following sections. The distribution generally corresponds to annual precipitation and runoff patterns. However, due to the effect of accumulation of water as it moves through the river channel network, higher discharge values occur downstream in large rivers.

### Table 1 Continental runoff (km³ /year)

| Region | UN (1997) | UNH (2000) | This study |
|---|---|---|---|
| Africa | 4,050 | 4,520 | 3,616 |
| Asia | 13,510 | 13,700 | 9,385 |
| Europe | 2,900 | 2,770 | 2,191 |
| Oceania | 2,404 | 714 | 1,680 |
| North America | 7,890 | 5,890 | 3,824 |
| South America | 12,030 | 11,700 | 8,789 |
| Total | 42,784 | 39,394 | 29,485 |

For the examination of the reliability of the results, annual runoff, before being routed through the river network, was compared with other estimates shown in Table 1. Detailed comparisons with observed discharge which can be found in a previous study (Oki et al., 1999) clearly revealed that the accuracy of the discharge estimates depends on the accuracy of forcing data, which can be inferred from the density of rain gauges.

From the runoff $R$ estimated based on the LSMs and river discharge $D$ after routing, water availability $Q$ in each grid box can be calculated as:

$$Q = R + \alpha \Sigma D_{up} \tag{7}$$

where $D_{up}$ is the river discharge from a grid box upstream and $\Sigma D_{up}$ denotes the sum of the discharges. The term $\alpha$ is the ratio indicating how much water from outside of the region (grid box) contributes

to water resources within the grid box. The same concept can be applied to the water availability estimation in countries. In this case, $\Sigma D_{up}$ corresponds to the transboundary water through natural river systems. The values listed in Table 1 correspond to the case when $\alpha = 0.0$, and the discharge in Fig. 1 at each grid box corresponds to $\alpha = 1.0$. The sensitivity showing how $\alpha$ affects water stress assessments will be examined in Section 4.

**Table 2  Country statistics used for estimating annual water withdrawal (from WRI CD-ROM)**

| Data | Unit | Year | Source |
|------|------|------|--------|
| Total withdrawal | km$^3$ | 1970-1995 | Various |
| Sectoral withdrawal | % | 1970-1995 or 1987 | WRI |
| Desalinated water | $10^6$ m$^3$ | 1990 | FAO |
| Population | $10^3$ | 1950-2050 | UN |
| Irrigated Area | $10^3$ ha | 1961-1994 | FAO |
| GDP per capita | US$ in 1995 | 1970-1995 | WB |

# 3 Water demand estimated using G-GIS

Statistics related to water withdrawal (demand side) were given in each country and obtained from the CD-ROM of the World Resources Institute (WRI *et al.*, 1998).

As can be seen, the years in the statistics of total/sectoral withdrawal were not unified and some adjustment was required to standardize the years. In this study, linear trends between 1970 and 1995 were assumed for each continent and estimated from Shiklomanov (2000b). Due to the limitations in available information, it was also assumed that the share of water withdrawal did not change during the period.
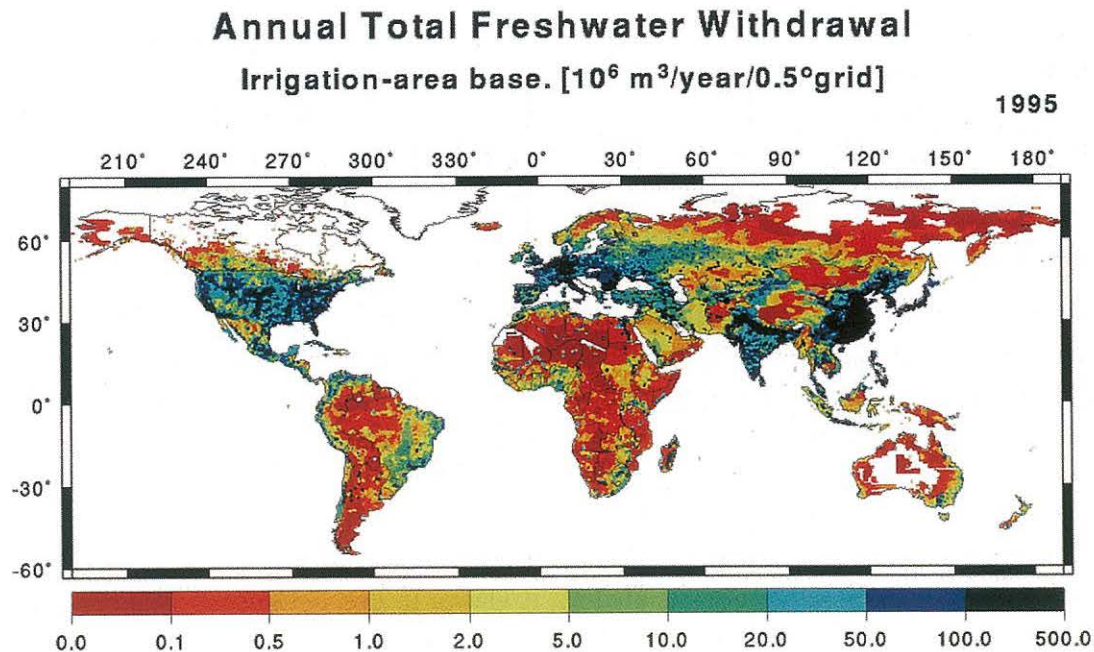


**Annual Total Freshwater Withdrawal**
Irrigation-area base. [$10^6$ m$^3$/year/0.5°grid]
1995

**Fig. 2  Estimated global distribution of annual water withdrawal in 1995**

In order to distribute the annual water withdrawal given by country statistics, a global geographical

information system (GIS)-based approach was adopted. The gridded (raster) data are summarized in Table 2. Population data were taken from CIESIN (Center for International Earth Science Information Network), and irrigation area from Kassel University (Doll and Siebert, 1999), and vector country boundary from ESRI (Environmental Systems Research Institute).

Firstly, templates for each country were generated on 0.5° by 0.5° lat./lon. grid boxes using a geographical information system, and small modifications were applied to fit to the situation in 1995, since some national boundary changes occurred after the release of the data from ESRI. The country area sizes on the 0.5° by 0.5° lat./lon. grid were calculated considering the ellipsity of the earth (Oki and Sud, 1998) and compared with national statistics. The mean of bias error was 5% and standard deviation was 32%.

The population distribution given in 2.5′ global grids was transferred to 0.5° by 0.5° lat./lon. grids. However, it was found that the total population after the conversion was less than the actual one by nearly 300 million people. This is because each 0.5° by 0.5° grid box was considered to be the ocean if more than half of the grid boxes corresponded to the ocean. However, there were some 2.5′ by 2.5′ grid boxes with inhabitants. This problem was solved by putting the population within sea grid boxes onto the nearest land grid boxes. Consequently, the results could be well compared with national statistics by 1% of mean bias error and 14% of standard deviation error.

Irrigation area data were provided by Doll and Siebert (1999). The spatial resolution and the target year correspond to those of the current study. Even though the dataset was estimated based on FAO (Food and Agriculture Organization) statistics, the accumulated irrigation areas for each country were found to be smaller than those of FAO with a 12% mean bias error. Most of the error occurred in African countries. Further examination of these data will be necessary particularly for the assessment of future water withdrawal estimates.

Based on these global distributions of population and irrigated area, the national-level statistics using the unit withdrawal of municipal and industrial water use per capita, and agricultural water withdrawal per irrigated area were used to estimate the global distribution of water withdrawals.

The total annual water withdrawal ($10^6$ m³ / y / 0.5° x 0.5° ) is illustrated in Fig. 2. The water withdrawal was concentrated in urban areas in industrialized countries where the population density is high. Irrigated area corresponded to the populated areas in China and India, and the estimated water withdrawals in those countries were as large as those in the United States and European countries.

# 4 Global Water Resources Assesment

For the assessment of water scarcity in this study, the index used by UN *et al.* (1997) and Vorosmarty *et al.* (2000) was adopted, that is the ratio of the annual water withdrawal $W$ to the available annual water $Q$. According to Heap *et al.* (1998), the parameter desalinated water resources $S$ was subtracted from $W$, and the water scarcity index $R_{ws}$ was derived as:

$$R_{ws} = \frac{W-S}{Q} \qquad (8)$$

where $Q$ and $W$ are taken from the results given in Sections 2 and 3, and illustrated in Figs. 1 and 2, respectively. The global distribution of estimated $R_{ws}$ is shown in Fig. 3. Generally the severity of water scarcity is estimated as:

$$
\begin{array}{llll}
 & R_{ws} & < 0.1 & \text{no water stress} \\
0.1 \leq & R_{ws} & < 0.2 & \text{low water stress} \\
0.2 \leq & R_{ws} & < 0.4 & \text{moderate water stress} \\
0.4 \leq & R_{ws} & & \text{high water stress}
\end{array}
$$

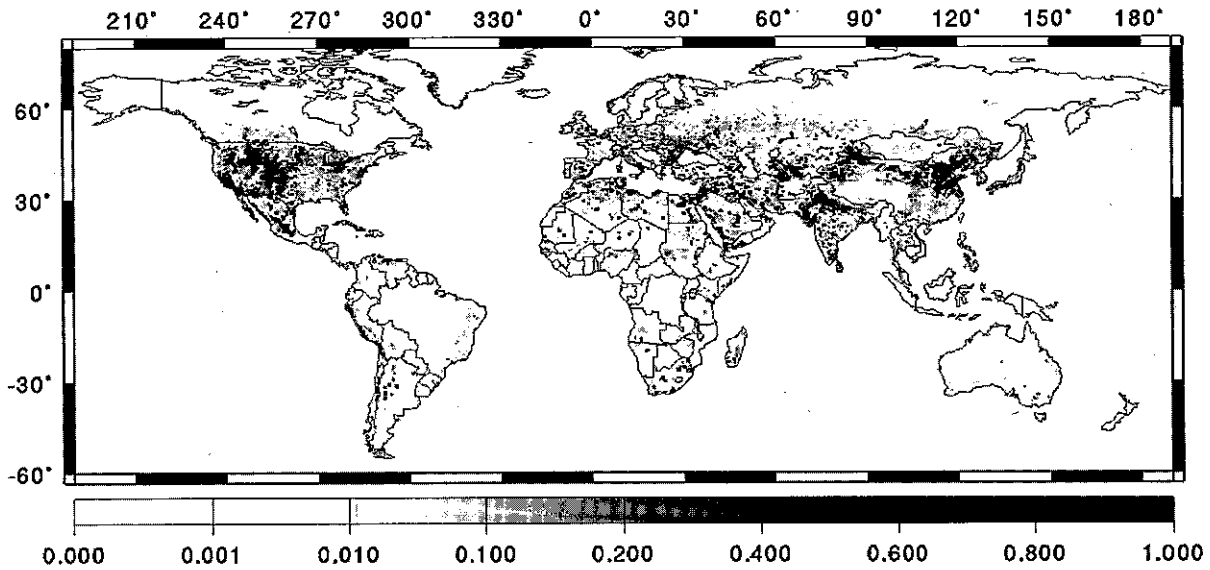# Annual Withdrawal to Availability Ratio

## ( W - S ) / Q

### 1995



Fig. 3   Global distribution of the water withdrawal to availability ratio in 1995

Following these criteria, it is evident from Fig. 3 that water scarcity was severe in the river basins of the Yellow, Indus, Ganges, and Amu-Darya, and in the middlewestern area of the United States. In these regions, the share of agricultural water withdrawal is generally high.
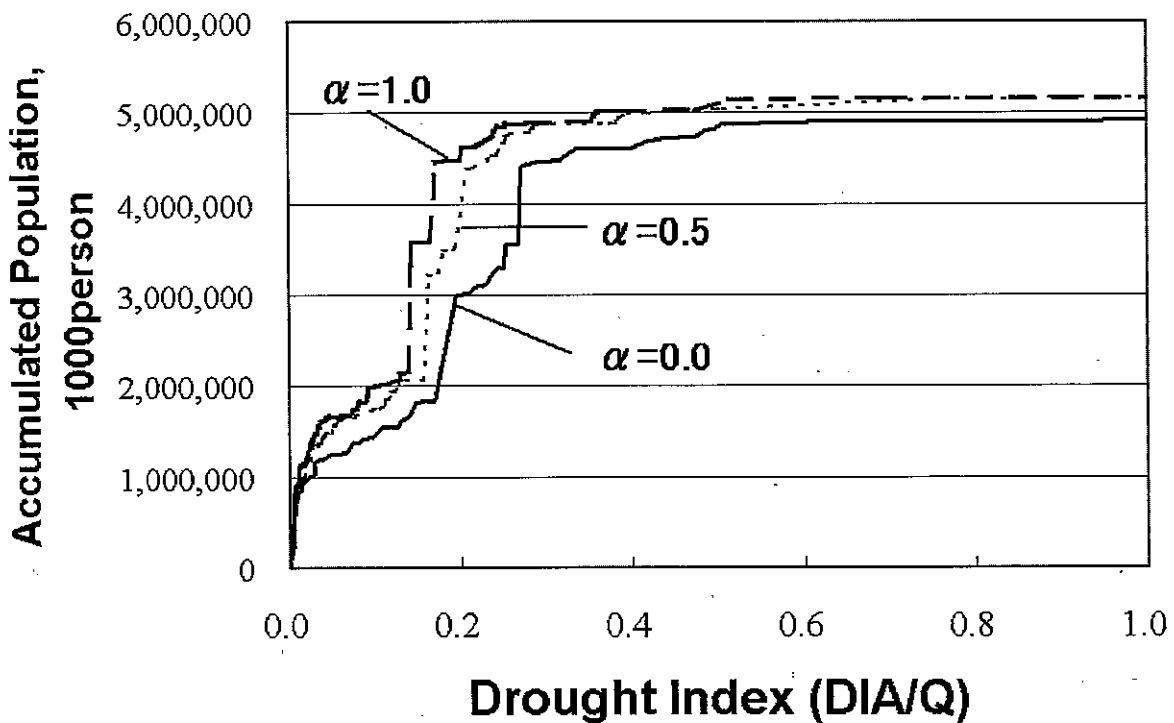


Fig. 4   Effect of $\alpha$ ratio on water stress assessment on a country basis

The estimated water scarcity was compared with data from previous studies (UN *et al.* (1997); Vörösmarty *et al.* (2000)) as shown in Table 3. The term $\alpha$ stands for the ratio indicating how much water from outside of the region (country or grid box) can be used (equation (8)). The current assessment results correspond well to previous results when $\alpha$ =0.5 was assumed. Moreover, it is noticeable that the estimate highly depends on the $\alpha$ value shown in Fig. 4. The number of people (ordinate) affected by water stress below the water withdrawal to availability ratio $R_{ws}$ (abscissa) clearly depends on the availability of water from outside of the region, which is represented by the $\alpha$ value. Figure 4 implicitly suggests that the availability of transboundary water exerts a great influence on the global assessment of water scarcity, and more detailed studies should be carried out on this issue.

**Table 3   Comparison of the population ($10^8$ capita) under levels of water scarcity on grid, country, and river basin basis**

| $Rws$ | Country basis | | | | | | Grid basis | | River basis |
|---|---|---|---|---|---|---|---|---|---|
| | TRIP | | | | UNH | UN | TRIP | UNH | TRIP |
| $\alpha$ | 0.0 | 0.5 | 1.0 | 1.0* | 1.0 | 1.0 | 1.0 | 1.0 | 0.0 |
| $R_{ws}< 0.1$ | 15 | 17 | 18 | 18 | 20 | 17 | 28 | 32 | 12 |
| $0.1 \le R_{ws}< 0.2$ | 2 | 3 | 3 | 15 | 17 | 21 | 6 | 4 | 5 |
| $0.2 \le R_{ws}< 0.4$ | 17 | 27 | 27 | 15 | 15 | 14 | 6 | 4 | 12 |
| $0.4 < R_{ws}$ | 22 | 9 | 8 | 8 | 5 | 5 | 17 | 18 | 27 |

UN: UN and other organizations (UN *et al.*, 1997).
UNH: University of New Hampshire (Vörösmarty *et al.*, 2000).
TRIP: This Study.
$R_{ws}$ : Water scarcity index.
$\alpha$ : Availability of water resources originating outside from the region.
TRIP and $\alpha$ =1.0* case can be applied if China ($R_{ws}$=0.26) is classified as $0.1 \le R_{ws}< 0.2$.

As pointed by Vörösmarty *et al.* (2000), the population under high water stress and also the population under no water stress are much higher, based on grid estimates, because averaging over a country eliminates the differences in water withdrawal and supply which occur spatially. Consequently, $R_{ws}$ will be underestimated. The evaluation of water scarcity in each river basin shows the largest population under severe water stress because $\alpha$ is assumed to be zero for this case, and no water from upstream is considered to be available downstream for water resources. Actually, the recycling ratios of water withdrawn for agriculture, industry, and municipal use are estimated at 25%, 86%, and 60%, respectively. Considering that the share of annual water withdrawal for these water uses is 69%, 23%, and 8%, respectively (WRI *et al.*, 1998), the mean recycling ratio could be estimated at 42%. Therefore, in order to assess more realistically the situation of future global water resources, a new approach to route the natural runoff generated in each grid by considering of water withdrawal and return flow in the grid box should be adopted.

# 5 Future projections

Projections of water resources and water scarcity for the year 2050 were carried out, considering the effects of climate change and population growth in order to investigate the changes in the severity of the water crisis in the near future. Although several scenarios were considered, we present the results of one scenario here.

The changes in the global discharge were calculated as follows. The results of a global warming climate

simulation using a general circulation model were obtained from the Center for Climate System Research, University of Tokyo. The global warming climate simulation was carried out with a fine resolution and consisted of a simulation under the current conditions and a simulation under global warming conditions. Then, the difference in the runoff from the land surface model in the climate simulation between the global warming simulation and the current simulation was calculated, and interpolated into 0.5° grid resolution which corresponded to the TRIP resolution. The interpolated runoff difference was added to the runoff from the LSMs described in the second Section so that the TRIP-based global discharge in 2050 was produced.



# Annual Withdrawal to Availability Ratio
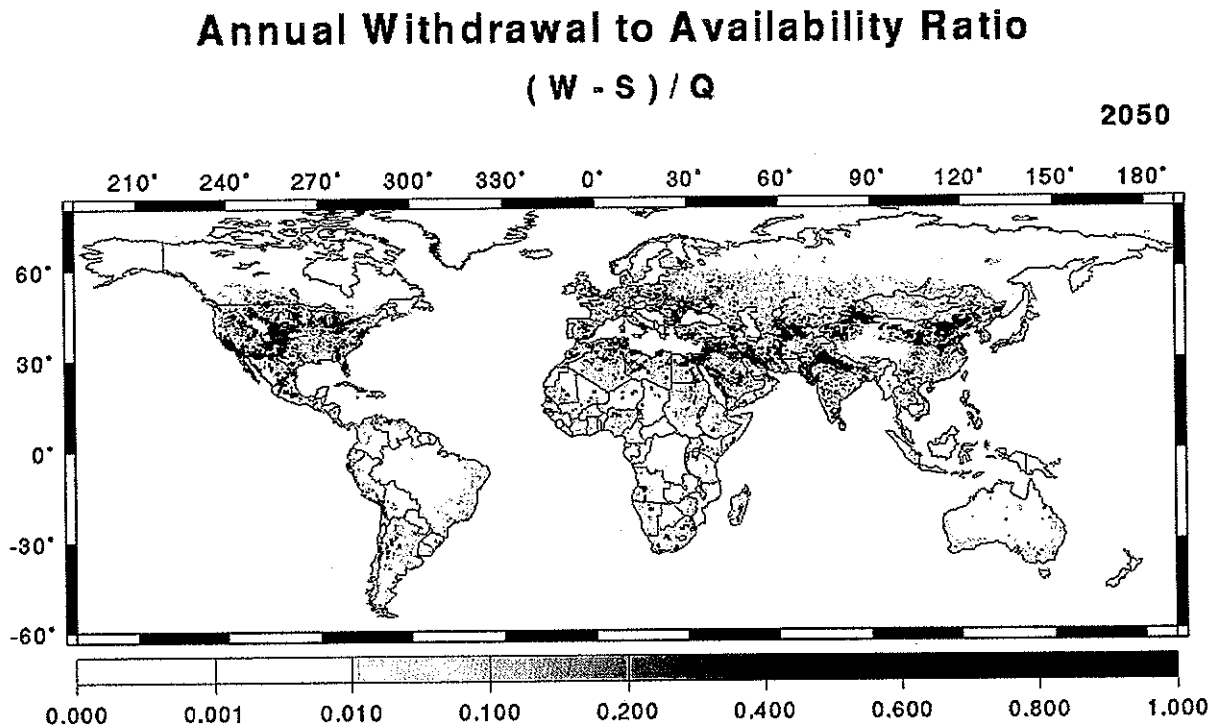## ( W - S ) / Q
**2050**

Fig. 5 Global distribution of the water withdrawal to availability ratio in 2050

The population growth was taken from the estimate by the United Nations. Since we assumed that the unit water withdrawal per capita for industrial use and municipal use would not change in the near future, the population change should affect the total industrial and municipal water withdrawal in a grid or in a region. The population change affects agricultural water withdrawal as well. The distribution of the agricultural water withdrawal in 1995 was calculated using the irrigation area data, as indicated in the third Section. For the future projections, a linear relationship between the global irrigation area and the global population was observed, when we examined the historical relationship between the global irrigation area and the global population, so that the changes in irrigation areas in the future could be estimated using the population change. The unit water withdrawal for agriculture was assumed to remain unchanged. Thus, the geographically distributed estimate of agricultural water withdrawal in the future was determined.

Since both the global discharge in 2050 and the water demand in the future were estimated as indicated above, the grid-based water scarcity ratio in 2050 was calculated (Fig. 5). The changes in the distribution of water stress between 1995 and 2050 did not seem to be apparent at a glance, based on the two figures for 1995 and 2050. Therefore, the distribution of the changes in the water scarcity ratio between 1995 and 2050 is shown in Fig. 6. It appears that the regions with severe stress in 1995 will still experience severe stress in the projection for 2050 and the severity will even increase in most regions. The regions with severe stress will

also spread to the neighboring areas. Such regions with increased water scarcity are mostly located in developing countries. The increase of discharge associated with global warming can mitigate the water scarcity in some regions. However, the effect of the population growth compensates such mitigation, or even increases the severity in such regions. The worse situation can be seen in the developing regions with a high population growth rate and with a decreased discharge under global warming conditions. As a whole, the effect of population change will be the major factor contributing to the increased severity of water scarcity in the future.
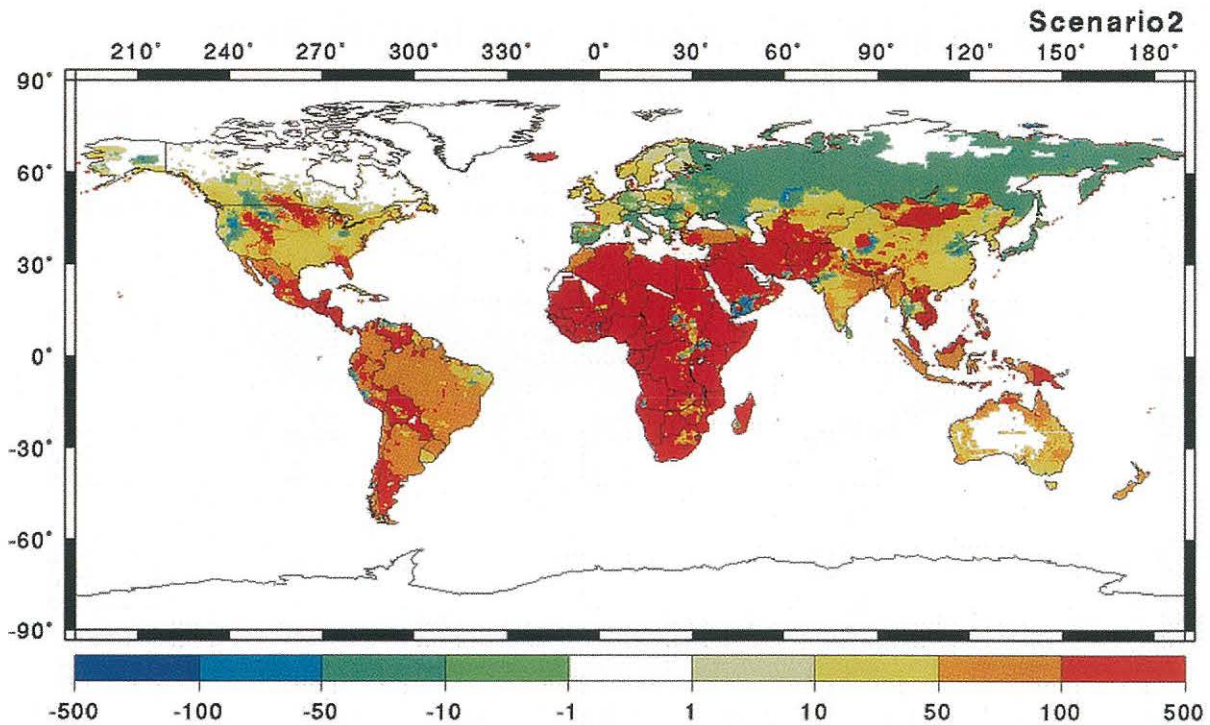


**Fig. 6  Global distribution of the changes in the water scarcity ratio between 1995 and 2050 Unit/percentage**

The time series of the water scarcity ratio for selected river basins (Fig. 7) was investigated for the regional water resources assessment. The severity of water scarcity for the Danube basin did not change appreciably in the time series from the current situation to 2050, presumably because of the stable society and population in such a comparatively mature basin. The Yellow River basin in China now experiences water scarcity. Generally it is anticipated that water scarcity may increase in the future in the Yellow River basin. However, the changes in the water scarcity ratio were projected to be considerably less pronounced than what was anticipated. The small increase in the water scarcity ratio was partly due to the limited population growth and partly due to the mitigation by global warming. The situation in the Indus basin will become severe with a linear increase mainly due to the continuous population growth.

# 6 Summary

Water availability and water withdrawal were estimated globally in 0.5° by 0.5° lon./lat. grid boxes, and water stress distribution was discussed. Summary for each continent is shown in Table 3.

Even though the amount of available water in Asia is large, population and current water withdrawal,

particularly agricultural water demand are very high, and the water stress ratio is the highest among the continents.

A water resources assessment in the future under the influence of global warming and population change was also carried out. Intensified water scarcity was found mainly in and close to the regions of water scarcity under the current conditions. The population growth in the future will exert a major effect on the severity of water scarcity compared to climate change.

The estimation of water availability was based on an offline simulation using land surface models and partly by a climate model for the future assessment. Efforts to improve the accuracy should be associated with the application of a higher temporal resolution, etc. The seasonal mismatch between the water demand and water availability should be considered in the water resources assessment even on a global scale.

Global assessment of $\alpha$ is necessary for robust estimates of water scarcity, and the influence of pollution can be included in the term $\alpha$ since the polluted water should be excluded from the "available" water resources in the assessments.
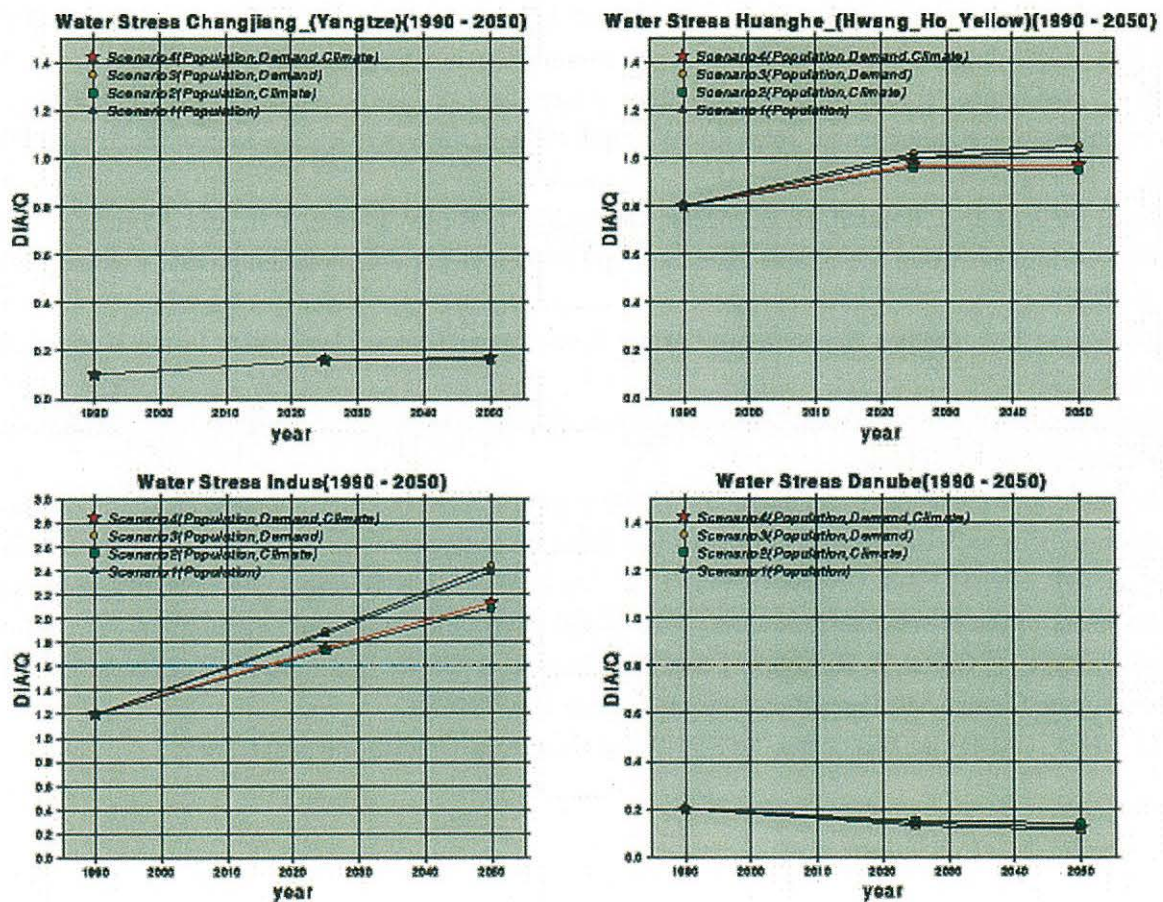


Fig. 7 Changes in water scarcity in selected basins

# References

1) Arora, V. K., Chiew, F. H. S. and Grayson, R.B. (1999): A river flow routing scheme for general circulation models. J. Geophys. Res. 104, 14347-14357.

2) Döll, P. and Siebert, S. (1999): A Digital Global Map of Irrigated Areas. Report a9901, Center for

Environmental System Research, University of Kassel.

3) Heap, C., Kemp-Benedict, E. and Raskin, P. (1998): Conventional Worlds: Technical Description of Bending the Curve Scenarios. Polestar Series Report.

4) IGPO (1995): Global Soil Wetness Project. Technical report, International GEWEX Project Office, Silver Spring, MD 20910.

5) Leopold, L. B. (1996): A View of the River. Vol.4, Harvard University Press.

6) Manabe, S. (1969): Climate and the ocean circulation. I. The atmospheric circulation and the hydrology of the earth's surface. Mon. Wea. Rev. 97, 739-774.

7) Meeson, B. W., Corprew, F. E., McManus, J. M. P., Myers, D. M., Closs, J. W., Sun, K.-J., Sunday, D. J. and Sellers, P. J. (1995): ISLSCP Initiative I - Global Data Sets for Land-Atmosphere Models, 1987-1988., Published on CD-ROM by NASA (USA_NASA_GDAAC_ISLSCP_001 - USA_NASA_GDAAC_ISLSCP_005).

8) Numaguti, A., Sugata, S., Takahashi, M., Nakajima, T. and Sumi, A. (1997): Study on the climate system and mass transport by a climate model. CGER's Supercomputer Monograph Report (ed. by National Institute for Environmental Studies, Environment Agency of Japan) 3

9) Oki, T. and Sud, Y. C. (1998): Design of Total Runoff Integrating Pathways (TRIP) - A global river channel network. Earth Interactions 2, [Available on-line at http://EarthInteractions.org/].

10) Oki, T., Nishimura, T. and Dirmeyer, P. (1999): Assessment of Land Surface Models by runoff in major river basins of the globe using Total Runoff Integrating Pathways (TRIP). J. Meteor. Soc. Japan 77, 235-255.

11) Sato, N., Sellers, P. J., Randall, D., Schneider, E., Shukla, J., Kinter, J., Hou, Y.-T. and Albertazzi, E. (1989): Effects of Implementing the Simple Biosphere Model in a General Circulation Model. J. Atmosp. Sci. 31, 1791-1806.

12) Shiklomanov, I. A. (2000a): Assessment of Water Resources and Water Availability in the World. UNESCO, Paris, France.

13) Shiklomanov, I. A. (2000b): World Water Resources: Modern Assessment and Outlook for the 21st Century. IHP/UNESCO, Paris, France.

14) Takahashi, K., Matsuoka, Y., Shimada, Y. and Shimamura, R. (2000): Development of the model to assess water resources problems under climate change. Proc. 8th Symposium on Global Environment 8, 175-180.

15) UN, UNDP, UNEP, FAO, UNESCO, WMO, W. Bank, WHO, UNIDO and SEI (1997): Comprehensive Assessment of the Freshwater Resources of the World. World Meteorological Organization.

16) Vörösmarty, C. J., Green, P., Salisbury, J. and Lammers, R. B. (2000): Global Water Resources: Vulnerability from Climate Change and Population Growth. Science 289, 284-288.

17) WRI, UNEP, UNDP and WB (1998): 1998-99 World Resources. Oxford University Press.